Proceedings of the Indian National Science Academy (2023) 89:825–836
https://doi.org/10.1007/s43538-023-00196-4

RESEARCH PAPER

Common structural attributes of tyrosinase variants are unlikely to determine differential retentions within endoplasmic reticulum: a homology modelling study with 45 variants

Kausik Ganguly[1,3] · Tithi Dutta[1] · Sayak Ganguli[2] · Mainak Sengupta[1]

Received: 18 April 2023 / Accepted: 1 August 2023 / Published online: 29 August 2023

Abstract
Tyrosinase is the key enzyme (TYR) regulating melanin biosynthesis pathway and different TYR mutants had been shown to be retained within the Endoplasmic Reticulum (ER) in varying degrees, instead of being localized in the melanosome. Interestingly, a direct correlation could be ascertained between the enzyme activities of the mutants and their respective degrees of ER retentions (Moumita Chaki et al., 2011; Mondal, Sengupta, & Ray, 2016); but the molecular bases of such variations in retentions has largely been unknown. In the current study, for the very first time, we tried to check if structural constraints like—(i) position of an amino acid within TYR, whether buried or surface exposed (which is reflected by Accessible Surface Area value), (ii) change in nature of amino acid, (iii) changes in overall electrostatic potential (iv) changes in hydrogen bonding (v) steric hindrance (vi) change in overall stability due to non-synonymous amino acid substitutions have contributing effects upon differential retentions of the mutants within ER. To achieve our aim, we did homology models of 45 TYR variants that have previously been functionally characterized by Mondal, Sengupta, & Ray, 2016, with respect to their degrees of ER retentions, as well as their individual levels of enzyme activities. To our surprise, we did not get any correlations whatsoever between differential functional characteristics of mutant TYRs with differential structural attributes. This indicates towards the role of some hitherto unexplored mechanism of processing of mutant protein variants that contribute toward their differential functional outcomes.

Keywords Tyrosinase · Homology-model · ER-retention · Structural-parameters

Introduction

Mature Tyrosinase (TYR, monophenol monoxygenase EC 1.14.18.1, UniProt #14,679) is a melanosomal membrane-bound glycoenzyme with a type-3 copper active site. TYR undergoes extensive processing inside endoplasmic reticulum (ER) aided by the chaperones Bip, Calnexin and Calreticulin, from where, it reaches the Golgi and next the melanosomes, the site of its function and subsequent pigment production. Though mammalian TYR in its pure and complete form has not been crystallized yet, the domains of the protein are well characterized. Mature TYR harbours seven N-glycosylation sites; two copper binding sites (CuA and CuB) and one transmembrane (TM) domain followed by a relatively short carboxyl-tail that contains the essential signals for sorting and targeting to the melanosomes (Ray et al. 2007).

Based on previous studies, it has been implicated that OCA1 (OCA: Oculocutaneous Albinism, here Type 1),

✉ Mainak Sengupta
sengupta.mainak@gmail.com

Kausik Ganguly
kausikganguly6@gmail.com

Tithi Dutta
tithi613@gmail.com

Sayak Ganguli
sayakbif@yahoo.com

[1] Department of Genetics, University of Calcutta, UCSTA, 35, Ballygunge Circular Road, Kolkata, West Bengal 700019, India

[2] Department of Biotechnology, St. Xavier's College (Autonomous), 30, Mother Teresa Sarani, Kolkata, West Bengal 700016, India

[3] Present Address: Department of Pulmonary Medicine, IPGME&R, Kolkata, West Bengal 700020, India

caused by mutations in *TYR* (TYR encoding human gene, OMIM #606,933), is an ER-retention disorder (Halaban et al. 2000; Mondal et al., 2016; Toyofuku et al., 2001) and different degrees of retentions in ER was evident for different *TYR* variants precipitating either OCA1A or OCA1B (Francis et al., 2003; Halaban et al., 2000; Halaban et al., 2002; Mondal et al., 2016). It is important to mention here that any un/misfolded protein enters and re-enters the chaperone CNX/CRT (Calnexin/Calreticulin) cycle via UGGT (UDP-glucose: glycoprotein glucosyl transferase) pathway and if still fails to fold correctly even after repeated cycles of CNX/CRT binding, is sorted out to the cytosol by EDEM (ER degradation enhancing—mannosidase-like protein) for proteasomal degradation (Ray et al., 2007). Thus, until proteasomal degradation, the misfolded mutant protein remains bound to ER chaperones, as reflected by Endoglycosidase H (Endo-H) sensitive bands post Endo-H assay. OCA1 causing missense mutations like p.L9P, p.D42N, p.R52I, p.K131E, p.H202R, p.R239W, p.G295R were observed to be completely ER retained post Endo-H assays and having zero TYR activities; in contrast, p.G41R, p.S192Y, p.Y433C were found to be partially retained within ER and having residual TYR enzyme activities, while few other TYR variants like p.L6F, p.S79P, p.T325A, p.A490G were found retain wild type (WT) like enzyme activity, besides not being retained at-all within the ER lumen. Interestingly, p.S192Y and p.H202R residing within the same Copper A domain were found to be partially and completely retained within ER lumen, respectively, having different degrees of TYR enzyme activities as already mentioned (Chaki et al., 2011; Mondal et al., 2016). In view of all this information, we thought variant wise modulation of TYR's structural attributes might be the contributory factor towards different degrees of ER retentions for the different mutants. We thought of checking if the solvent accessibility of the mutant residue i.e. if the position of the variant residue within TYR protein are buried deep inside the TYR protein structure or are more of surface exposed kind and if that can be correlated with different degrees of ER retentions. Interestingly, previous studies (Sarkar et al. 2014; Sengupta et al. 2015) have shown that changes in hydrogen bonds with neighbouring residues, introduction of steric clash or weak bonds, changes in overall electrostatic potential maps are important parameters for a mutation to exert different degrees of "deleterious" effects on protein structure and/or functions, which may correlate with different degrees of severity of disease outcomes. Again, alteration of overall protein stability and torsional property have long been observed to contribute differential functions on mutated protein variants (Ahmed et al. 2022; Seifi & Walter 2018; Shafie et al. 2021). We thought these parameters too ought to be checked for TYR protein variants in understanding the molecular basis of differential degrees of ER retentions. In accordance, we modelled TYR WT and mutated protein variants and compared the above-mentioned structural attributes between WT and the mutated TYR protein variant models.

Materials and methods

Generation of homology model for wild type tyrosinase protein

Due to the unavailability of crystal structure of purified human tyrosinase protein, a homology model was generated using the crystal structure of *Bacillus megaterium* tyrosinase (PDB Id: 3NM8) as template and primary sequence of human Tyrosinase (UniProt Id: P14679) as input sequence. Primary sequence of 3NM8 was found to have 28.95 percent identical residues with that of P14679, whereas 93% of the amino acid residues of 3NM8 were covered by P14679. Secondary structural propensities were evaluated based on standard Chou Fasman parameters (Chou & Fasman 1974) and the putative secondary structures were determined prior to modeling using the GOR algorithm (Garnier et al. 1978). The homology modeling was done using Modeller (Webb & Sali 2016). The modeled structure was further simulated using GROMOS96 43a2 force field using 40 ns simulation option of Gromacs (Abraham et al. 2015; Berendsen et al. 1995). Using the MOLPROBITY server (Chen et al. 2010) the best possible modeled homology structure was analyzed for torsional/conformational stability. The integrity and validity of the 3D model generated was verified by the associated Q-MEAN score. It is to be mentioned here that more the Q-MEAN score, more it is suited for further structural analyses.

Generation of mutant structures from wild type homology model

All the 45 TYR variants (see Table 1) checked functionally in Mondal et al., 2016 study, one of the most comprehensive functional studies conducted on OCA causing TYR mutants, were used for generation of mutant models using Deep View-Swiss-PDB-viewer tool (Guex & Peitsch 1997) and simulated using Gromacs (Abraham et al. 2015; Berendsen et al. 1995), as already mentioned.

Structural analyses using chimera, deep view-swiss-PDB-viewer and CUPSAT

In order to check the torsional distortion and structural comparison between WT Tyrosinase model and respective mutant models, each mutant model was separately superimposed using the MatchMaker option of UCSF-Chimera (Pettersen et al. 2004) and respective RMSD (Root Mean

Table 1 Summarized table of structural attributes of the TYR mutants assessed using Chimera, Deep View-Swiss-PDB-viewer and CUPSAT

Tyrosinase variants [1]	Retention degree in ER (Mondal et al. 2016) [2]	RMSD from UCSF chimera [3]	Nature of substitution [4]	Structural analyses done in deep view-swiss-PDB-viewer			Structural analyses done in CUPSAT			
				Change in overall electrostatic potential map [5]	Change in hydrogen bonding to adjacent residues [6]	Introduction of steric clash [7]	Overall Stability prediction-thermal method [8]	Torsion prediction-thermal method [9]	Overall Stability prediction-denaturants method [10]	Torsion prediction-denaturants method [11]
p.L9P	Total	0.019	Non-polar to non-polar	No	No	Yes	Destabilizing	Unfavourable	Stabilizing	Unfavourable
p.R52I	Total	0.001	Positively charged to non-polar	Yes	Yes	No	Stabilizing	Favourable	Stabilizing	Favourable
p.K131E	Total	0.002	Positively charged to negatively charged	Yes	Yes	No	Stabilizing	Favourable	Stabilizing	Favourable
p.R239W	Total	0.004	Positively charged to non-polar	Yes	Yes	No	Destabilizing	Favourable	Destabilizing	Favourable
p.G295R	Total	0.001	Non-polar to positively charged	No	No	No	Stabilizing	Unfavourable	Destabilizing	Unfavourable
p.P81S	Total	0.001	Non-polar to polar	No	No	No	Destabilizing	Favourable	Stabilizing	Favourable
p.F84V	Total	0.001	Non-polar to non-polar	No	No	No	Destabilizing	Unfavourable	Stabilizing	Unfavourable
p.G97V	Total	0.001	Non-polar to non-polar	No	No	No	Destabilizing	Unfavourable	Stabilizing	Unfavourable
p.K142M	Total	0.035	Positively charged to non-polar	Yes	Yes	Yes	Stabilizing	Favourable	Destabilizing	Favourable
p.H202R	Total	0.008	Positively charged to positively charged	Yes	Yes	No	Stabilizing	Unfavourable	Stabilizing	Unfavourable
p.P209R	Total	0.055	Non-polar to positively charged	Yes	No	No	Stabilizing	Favourable	Stabilizing	Favourable
p.Y327C	Total	0.001	Polar to non-polar	No	Yes	Yes	Destabilizing	Unfavourable	Stabilizing	Unfavourable
p.M332T	Total	0.001	Non-polar to polar	No	Yes	No	Stabilizing	Favourable	Stabilizing	Favourable
p.N371Y	Total	0.004	Polar to polar	No	Yes	Yes	Destabilizing	Unfavourable	Stabilizing	Unfavourable

Table 1 (continued)

Tyrosinase variants [1]	Retention degree in ER (Mondal et al. 2016) [2]	RMSD from UCSF chimera [3]	Nature of substitution [4]	Structural analyses done in deep view-swiss-PDB-viewer			Structural analyses done in CUPSAT			
				Change in overall electrostatic potential map [5]	Change in hydrogen bonding to adjacent residues [6]	Introduction of steric clash [7]	Overall Stability prediction-thermal method [8]	Torsion prediction-thermal method [9]	Overall Stability prediction-denaturants method [10]	Torsion prediction-denaturants method [11]
p.R422W	Total	0.001	Positively charged to non-polar	Yes	Yes	Yes	Destabilizing	No change	Stabilizing	No change
p.P21L	Total	0.014	Non-polar to non-polar	No	No	Yes	Destabilizing	Unfavourable	Stabilizing	Unfavourable
p.D42N	Total	0.032	Negatively charged to polar	Yes	No	No	Stabilizing	Unfavourable	Stabilizing	Unfavourable
p.C91S	Total	0.001	Non-polar to polar	No	Yes	No	Destabilizing	Favourable	Destabilizing	Favourable
p.V177D	Total	0.001	Non-polar to negatively charged	Yes	Yes	No	Destabilizing	Unfavourable	Stabilizing	Unfavourable
p.A206T	Total	0.001	Non-polar to polar	No	No	No	Destabilizing	Unfavourable	Stabilizing	Unfavourable
p.E219K	Total	0.039	Negatively charged to positively charged	Yes	Yes	No	Destabilizing	Favourable	Stabilizing	Favourable
p.G372R	Total	0.001	Non-polar to positively charged	Yes	Yes	No	Destabilizing	Favourable	Destabilizing	Favourable
p.T373L	Total	0.001	Polar to non-polar	No	No	No	Stabilizing	Unfavourable	Destabilizing	Unfavourable
p.Y411H	Total	0.074	Polar to positively charged	No	No	Yes	Destabilizing	Unfavourable	Destabilizing	Unfavourable
p.G419R	Total	0.001	Non-polar to positively charged	Yes	No	No	Destabilizing	Favourable	Destabilizing	Favourable
p.P45T	Total	0.001	Non-polar to polar	No	No	No	Stabilizing	Favourable	Destabilizing	Favourable
p.F134C	Total	0.001	Non-polar to non-polar	No	Yes	No	Destabilizing	Unfavourable	Stabilizing	Unfavourable
p.K142N	Total	0.034	Positively charged to polar	Yes	Yes	Yes	Stabilizing	Unfavourable	Destabilizing	Unfavourable

Table 1 (continued)

Tyrosinase variants [1]	Retention degree in ER (Mondal et al. 2016) [2]	RMSD from UCSF chimera [3]	Nature of substitution [4]	Structural analyses done in deep view-swiss-PDB-viewer			Structural analyses done in CUPSAT			
				Change in overall electrostatic potential map [5]	Change in hydrogen bonding to adjacent residues [6]	Introduction of steric clash [7]	Overall Stability prediction-thermal method [8]	Torsion prediction-thermal method [9]	Overall Stability prediction-denaturants method [10]	Torsion prediction-denaturants method [11]
p.D199N	Partial	0.033	Negatively charged to polar	No	Yes	No	Destabilizing	Unfavourable	Destabilizing	Unfavourable
p.G346V	Partial	0.001	Non-polar to non-polar	No	Yes	Yes	Destabilizing	Unfavourable	Destabilizing	Unfavourable
p.G41R	Partial	0.001	Non-polar to positively charged	Yes	Yes	No	Stabilizing	Unfavourable	Stabilizing	Unfavourable
p.Y433C	Partial	0.001	Polar to non-polar	Yes	Yes	No	Destabilizing	Favourable	Stabilizing	Favourable
p.C35R	Partial	0.001	Non-polar to positively charged	Yes	Yes	No	Destabilizing	Favourable	Destabilizing	Favourable
p. Q56H	Partial	0.002	Polar to positively charged	No	No	Yes	Stabilizing	Unfavourable	Stabilizing	Unfavourable
p.R239Q	Partial	0.047	Positively charged to polar	Yes	Yes	No	Destabilizing	Favourable	Stabilizing	Favourable
p.P260L	Partial	0.029	Non-polar to non-polar	No	No	No	Destabilizing	Unfavourable	Stabilizing	Favourable
p.A266T	Partial	0.001	Non-polar to polar	No	Yes	No	Stabilizing	Favourable	Stabilizing	Favourable
p.R308T	Partial	0.001	Positively charged to polar	Yes	No	No	Destabilizing	Unfavourable	Stabilizing	Unfavourable
p.A490G	Similar to WT	0.001	Non-polar to Non-polar	No	No	No	Destabilizing	Unfavourable	Stabilizing	Unfavourable
p.S79P	Similar to WT	0.001	Polar to non-polar	No	Yes	Yes	Stabilizing	Unfavourable	Stabilizing	Unfavourable
p.T325A	Similar to WT	0.002	Polar to Non-polar	No	Yes	No	Destabilizing	Unfavourable	Stabilizing	Unfavourable
p.L6F	Similar to WT	0.094	Non-polar to non-polar	No	No	No	Destabilizing	Unfavourable	Stabilizing	Unfavourable
p.P38T	Similar to WT	0.001	Non-polar to polar	No	No	No	Stabilizing	Unfavourable	Stabilizing	Unfavourable

Table 1 (continued)

Tyrosinase variants [1]	Retention degree in ER (Mondal et al. 2016) [2]	RMSD from UCSF chimera [3]	Nature of substitution [4]	Structural analyses done in deep view-swiss-PDB-viewer			Structural analyses done in CUPSAT			
				Change in overall electrostatic potential map [5]	Change in hydrogen bonding to adjacent residues [6]	Introduction of steric clash [7]	Overall Stability prediction-thermal method [8]	Torsion prediction-thermal method [9]	Overall Stability prediction-denaturants method [10]	Torsion prediction-denaturants method [11]
p.D125Y	Similar to WT	0.005	Negatively charged to polar	Yes	Yes	No	Stabilizing	Unfavourable	Destabilizing	Unfavourable
p.L263I	Similar to WT	0.001	Non-polar to non-polar	No	No	No	Destabilizing	Favourable	Stabilizing	Favourable

Square Deviation) values were noted down. Following a previous study (Kufareva & Abagyan 2012), RMSD value of at least 2–3 Å was considered to reflect significant change in structural conformation of mutant TYR protein. Further, changes in nature of amino acid substitutions were checked from standard amino acid table. Change in overall electrostatic potentials, change in hydrogen bonding and introduction of steric clash (if any) upon amino acid substitutions were checked using available options of Deep View-Swiss-PDB-viewer (SPDBV) tool. After uploading a PDB file, a step of energy minimization was carried out in SPDBV using "Energy minimization" option available under "Tools" tab. Then, the concerned amino acid residue was selected from control panel and energy minimized surrounding amino acid residues were automatically selected by SPDBV which may have probable interactions with the residue concerned. Then, overall electrostatic potential, available hydrogen bonds along with steric clash (if any) were checked using "Compute electrostatic potential", "Compute H bonds" options, respectively, available under the same "Tools" tab. For mutating a particular amino acid residue, "Mutate" tab of SPDBV was used post energy minimization step (as already mentioned). Same steps of calculating electrostatic potential, hydrogen bonding with neighbouring residues along with steric clash (if any) were carried out for the mutant residue containing PDB files, too. Overall protein stability predictions and torsion predictions upon concerned amino acid substitutions were checked from CUPSAT (Parthiban et al. 2006) using the option "Predict Mutant Stability from Custom Protein Structures". CUPSAT (available at http://cupsat.tu-bs.de/) tries to assess effect of point mutations on respective protein stability using protein containing amino acid atom potentials in terms of torsion angle perturbations *i.e.* a gaussian apodization function is used to accommodate torsion angle perturbations, thus, alterations in protein environment specific mean force potentials are checked for each amino acid variants.

Changes in accessible surface area value assesses by ASA-view

Often, a change in amino acid within a protein structure makes the amino acid moiety involved, more or less accessible to the surface of the protein concerned which can be assessed by measuring the changes in accessible surface area values from proper in silico tools. Accessible surface area value is a measure of checking hydrophobicity of an amino acid residue i.e. fundamentally, more an amino acid is buried deep down within a protein, more hydrophobic it would be, on the other hand, more exposed an amino acid is on the protein surface, more hydrophilic should it be. In this study, ASA-View (available at http://dna00.bio.kyutech.ac.jp/asaview/) was consulted for checking the degree

of hydrophobicity or relative accessible surface area of an amino acid when compared with its mutant form. ASA-View provides values of accessible surface area of a given amino acid moiety (Ahmad et al. 2004) which made it possible to check if changes in accessible surface area values impart a significant role in differential retention of mutant TYR proteins within ER.

The pathway of analyses followed in the study is shown in Fig. 1.

Checking biasness in distribution of data through statistical testing

In order to check biasness in distribution of data among various groups of mutated protein variants that exert functional outcomes in forms of either being completely, partially, or not at all retained within ER lumen, as already mentioned, 2*3 and/or 2*2 Fisher tests were performed using vassarstats online tool (http://vassarstats.net/fisher2x3.html; http://vassarstats.net/tab2x2.html).

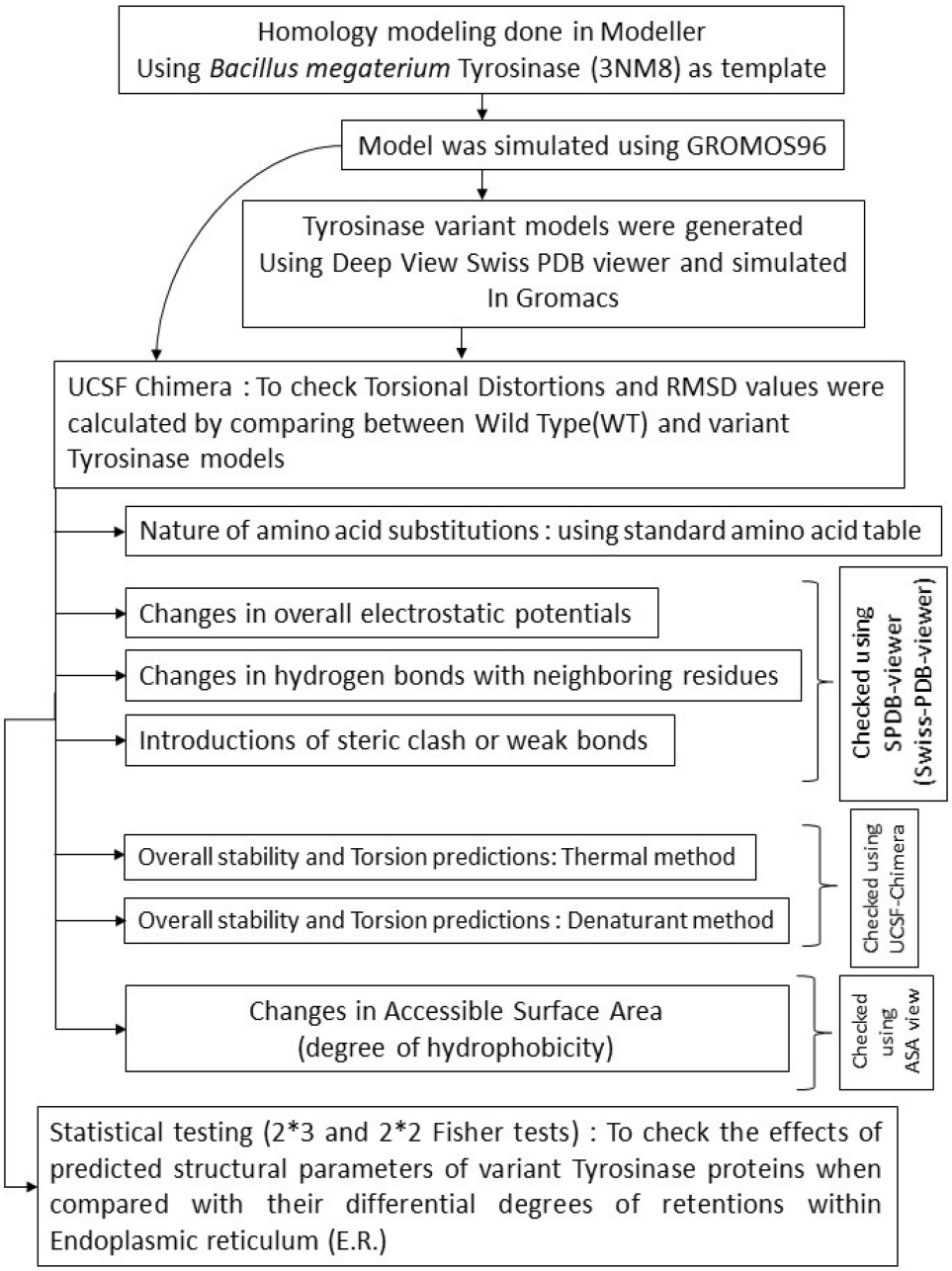

Fig. 1 Pathway of analyses followed to test hypothesis mentioned in the Introduction section. The hypothesis was that different degrees of retentions of mutant Tyrosinase proteins may occur due to their structural alterations brought about by the mutant amino acid variant. Due to unavailability of protein structure (complete structure of human Tyrosinase protein free from any ligand or any other molecule) file (X-ray diffraction or NMR generated) in Protein Data Bank, homology modelling was done based on *Bacillus megaterium* Tyrosinase (PDB accession ID: 3NM8) and different structural parameters were checked

Results

PDB structure of human Tyrosinase protein as modelled by Modeller and analysed by MOLPROBITY server is shown in Fig. 2. Downstream analyses were done upon this PDB structure using—(i) UCSF chimera, for RMSD value generations; (ii) Deep View-Swiss-PDB-viewer and (iii) CUPSAT for checking different structural parameters (Table 1). None of the variant structures modeled fetched any significant change in respective RMSD value as evident from Table 1, which is indicative of the fact that none of the replaced amino acids seemed to impart a significant angular distortion on the complete protein model when compared to WT protein structure. Further analyses were done to check if the nature (i.e. whether polar, non-polar, positively charged, negatively charged) of mutant amino acid residue had any significant role on the variable degrees of retentions in ER for the TYR mutants. Among 28 totally retrained mutant Tyrosinase proteins, 21 mutants had changes in their respective nature of amino acid (*e.g.* p.K131E, 'Positively charged' Lysine at 131st position, was substituted by 'Negatively charged' Glutamic acid and p.131E is a completely retained TYR variant) while for the other 7, no such change occurred (for p.L9P, Leucine and Proline, both are Non-polar amino acids). Similarly, when partially retained 10 mutant TYRs were considered, in case of 8 mutants, nature of amino acid was found to be altered. Finally, among the 7 variant TYRs which were found to behave like WT TYR protein (Mondal et al., 2016) when retentions within E.R. were considered, 4 were found to have non-conservative substitution. No significant bias ($p = 0.6277$) was found between non-conservative and conservative substitutions and degree of ER retention (Table 2). No significant bias ($p = 0.3619$) was found when completely retained and partially retained mutant proteins were clubbed together and compared to the ones not retained at all. Similarly, for none of the other structural parameters tested (i.e. changes in overall electrostatic potentials; changes in hydrogen bonding to surrounding residues; introduction of steric clash; protein stability predictions and changes in accessible surface area) checked for mutant TYR proteins (see Supplementary file 1), a significant correlation was found (see Tables 2, 3, 4, 5) with degree of ER retention.

Discussion

Previous studies had already shown that retention of mutant TYR within ER is the functional basis of precipitation of the rare genetic disorder—Oculocutaneous Albinism (Halaban et al., 2002; Halaban et al., 2000; Halaban et al., 1997; Toyofuku et al., 2001) and it has also been seen that different degrees of retentions of mutant TYR proteins within ER correlate with different levels of TYR enzyme activities

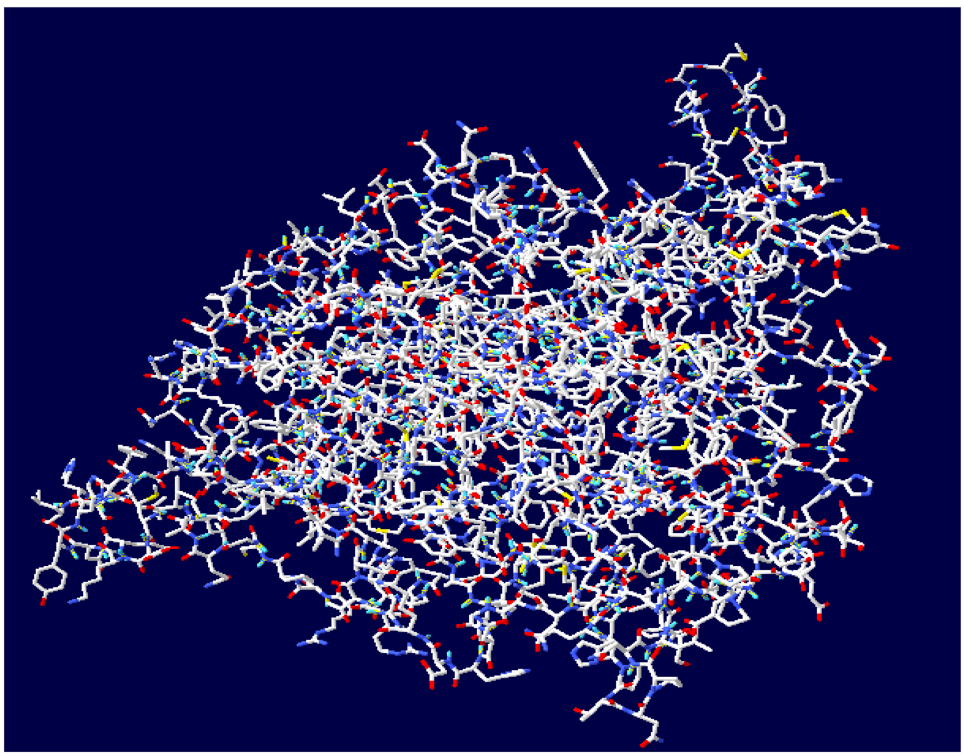

Fig. 2 The wild type homology model of human tyrosinase as viewed in Deep View-Swiss-PDB-viewer. All the 529 amino acid residues of modeled human Tyrosinase protein, are displayed in "render in solid 3D" view mode. (Colour guide—White: Carbon atom; Red: Oxygen atom; Blue: Nitrogen atom; Yellow: Sulphur atom; Cyan: Hydrogen atom)

Table 2 Statistical (2*3 and 2*2 Fisher test) distributions of the structural attributes checked using Deep View, when compared with their functional retention in ER data as reported by Mondal et al., 2016

Nature of ER retention (Mondal et al., 2016)	Change in nature of amino acid		Changes in overall electrostatic potential map		Changes in hydrogen bonds with neighbouring residues		Introduction of steric clash	
	Yes	No	Yes	No	Yes	No	Yes	No
Totally retained	21	7	13	15	15	13	8	20
Partially retained	8	2	5	5	6	4	3	7
Behaving like wild type	4	3	1	6	3	4	1	6
p-value of distribution	0.6277		0.3479		0.8344		0.7941	
Totally retained + Partially retained	29	9	18	20	21	17	11	27
Behaving like wild type	4	3	1	6	3	4	1	6
p-value of distribution	0.3619		0.2108		0.6886		0.6548	

Table 3 Statistical distributions (2*3 and 2*2 Fisher test) of the structural attributes checked using CUPSAT, when compared with their functional retention in ER data as reported by Mondal et al., 2016

Nature of ER retention (Mondal et al., 2016)	Overall stability prediction				Torsion prediction			
	Thermal method		Denaturant method		Thermal method		Denaturant method	
	Destabilizing	Stabilizing	Destabilizing	Stabilizing	Destabilizing	Stabilizing	Destabilizing	Stabilizing
Totally retained	17	11	10	18	15	13	15	13
Partially retained	7	3	3	7	6	4	5	5
Behaving like wild type	4	3	1	6	6	1	6	1
p-value of distribution	0.8267		0.661		0.3543		0.3479	
Totally retained + Partially retained	24	14	13	25	21	17	20	18
Behaving like wild type	4	3	1	6	6	1	6	1
p-value of distribution	1		0.4069		0.215		0.2108	

(Mondal et al., 2016) but sufficient proof in support of the functional basis of such differential retentions and differential degrees of enzyme activities of TYR protein, was scarce. Even though protein modeling studies has contributed to elucidate the deleterious outcomes of mutated protein variants of TYRP1in regulating OCA3 (Kamaraj & Purohit 2013), same kind of study has not been done for checking differential functional outcomes of TYR mutated variants. With our current study, for the very first time, we tried to decipher, through *molecular modelling* analyses, if differential retentions of mutant TYRs were contingent upon any structural parameter or not. It had been seen in case of mutant Factor VIII proteins that the severity of Haemophilia A is contingent upon the position of the affected residue within Factor VIII and their structural attributes (Sengupta et al., 2015). In another study of Sarkar et al. 2014, it was observed that fates of intracellular trafficking of different mutational variants of Connexin50 (CNX50) might be dependent upon significant changes in electrostatic potential maps upon mutation. Various other studies had also indicated that different structural attributes of mutated protein variants exert differential functional outcomes upon concerned protein structure, which in turn translate into differential protein functions and differences in disease etiology (Ahmed et al. 2022; Amir et al. 2019; Brewer et al. 2021; Seifi & Walter 2018; Shafie et al. 2021). However, our attempts with 45 TYR mutants and their degrees of ER retentions did not reveal any correlation with any of the locational or structural attributes of the mutant TYRs. The outcome discussed so far, could be a result of some other biological phenomenon which is yet to be unearthed, like changes in contact points between mutant TYR proteins and chaperones (or chaperone binding proteins), brought about by the altered amino acid on the three-dimensional stoichiometric structure of nascent TYR polypeptide, because chaperones are the immediate target of proteins once they come inside E.R. (Ray et al., 2007).

This should be mentioned here that homology or comparative modeling followed by simulation is always a predictive method for evaluating the structure of proteins which have not been crystalized. The template dependent methods often suffer from bias induced in the final structure of the protein due to the exact juxtaposition of the parameters of the template onto the subject and thus we find that native structures predicted using comparative/homology modeling often do

Table 4 Table of results for checking changes in relative accessible surface area values as procured from ASA-view

Tyrosinase variants	Retention in ER (Mondal et al., 2016)	Residue 1	ASA score of Residue 1	Residue 2	ASA score of Residue 2	Change in surface area (in percentage value)
p.L9P	Total	L9	0.513334	P9	0.366444	28.6148979
p.R52I	Total	R52	0.58941	I52	0.448615	23.88744677
p.K131E	Total	K131	0.111803	E131	0.131652	17.75354865
p.R239W	Total	R239	0.30562	W239	0.241164	21.09024279
p.G295R	Total	G295	0.31765	R295	0.685462	115.7915945
p.P81S	Total	P81	0.35235	S81	0.409536	16.22988506
p.F84V	Total	F84	0.657624	V84	0.624576	5.025364038
p.G97V	Total	G97	1	V97	0.982406	1.7594
p.K142M	Total	K142	0.009722	M142	0.029982	208.3933347
p.H202R	Total	H202	0.137425	R202	0.10915	20.57485901
p.P209R	Total	P209	0.07047	R209	0.048026	31.84901376
p.Y327C	Total	Y327	0.028074	C327	0.041634	48.300919
p.M332T	Total	M332	0.314811	T332	0.317196	0.757597416
p.N371Y	Total	N371	0.30052	Y371	0.304135	1.202914947
p.R422W	Total	R422	0.26196	W422	0.237006	9.525881814
p.P21L	Total	P21	0.239598	L21	0.185674	22.50603094
p.D42N	Total	D42	0.491675	N42	0.49176	0.017287843
p.C91S	Total	C91	0.353889	S91	0.264492	25.26131075
p.V177D	Total	V177	0.078072	D177	0.062325	20.16984322
p.A206T	Total	A206	0.027222	T206	0.014418	47.035486
p.E219K	Total	E219	0.011448	K219	0.004861	57.53843466
p.G372R	Total	G372	0.203296	R372	0.082954	59.19545884
p.T373L	Total	T373	0.057672	K373	0.038888	32.57039811
p.Y411H	Total	Y411	0.262024	H411	0.153916	41.25881599
p.G419R	Total	G419	0.216002	R419	0.279424	29.36176517
p.P45T	Total	P45	0.28188	T45	0.28836	2.298850575
p.F134C	Total	F134	0.02491	C134	0.013878	44.28743477
p.K142N	Total	K142	0.009722	N142	0.04781	391.7712405
p.D199N	Partial	D199	0.1662	N199	0.17758	6.847172082
p.G346V	Partial	G346	0	V346	0.013012	100
p.G41R	Partial	G41	0.965656	R41	0.32745	66.09040901
p.Y433C	Partial	Y433	0.037432	C433	0.027756	25.8495405
p.C35R	Partial	C35	0.353889	R35	0.554482	56.68246258
p.Q56H	Partial	Q56	0.128777	H56	0.115437	10.35899268
p.R239Q	Partial	R239	0.30562	Q239	0.235158	23.05542831
p.P260L	Partial	P260	0.549666	L260	0.693547	26.17607784
p.A266T	Partial	A266	0.027222	T266	0.021627	20.55322901
p.R308T	Partial	R308	0.733488	T308	0.814617	11.06071265
p.A490G	Similar to WT	A490	0.462774	G490	0.533652	15.31589934
p. S 79 P	Similar to WT	S79	0.25596	P79	0.218457	14.65189873
p.T325A	Similar to WT	T325	0.605556	A325	0.462774	23.57866159
p.L6F	Similar to WT	L6	0.633476	F6	0.652642	3.025528986
p.P38T	Similar to WT	P38	0.754029	T38	0.735318	2.481469546
p.D125Y	Similar to WT	D125	0.671725	Y125	0.449184	33.12977781
p.L263I	Similar to WT	L263	0.060071	I263	0.059455	1.025453214

Table 5 Statistical distributions (2*3 and 2*2 Fisher tests) of the structural attributes checked using ASA-View, when compared with their functional retention in E.R. data as reported by Mondal et al., 2016

Nature of E.R. retention (Mondal et al., 2016)	Change in relative surface area (as procured from ASA view)	
	0% to 50%	50% and beyond
Totally retained	23	5
Partially retained	7	3
Behaving like wild type	7	0
p-value of distribution	0.3352	
Totally retained + Partially retained	30	8
Behaving like wild type	7	0
p-value of distribution	0.3212	

not have biological functionality if they are experimentally obtained. However, this still remains as the best method for predicting structure function relationships and studies on interactions for cases where crystal structures still remain unattained.

Supplementary Information The online version contains supplementary material available at https://doi.org/10.1007/s43538-023-00196-4.

Author contributions KG, SG, MS: conceptualization and manuscript editing. KG: experimentation, data curation and analysis, manuscript writing. TD, SG: experimentation and data curation.

Funding The study was supported by departmental infra-structural support by Department of Science and Technology-Promotion of University Research and Scientific Excellence (DST PURSE), Government of India. K Ganguly was supported by Senior Research Fellowship (SRF) from DST-PURSE Programme Phase II (DST-PURSE-II SRF) at University of Calcutta and was later supported by Project Fellowship from DST-SERB, Government of India. T Dutta was supported by Junior Research Fellowship (JRF) and Senior Research Fellowship (SRF) from University Grants Commission (UGC), Government of India.

Data availability All data supporting this work had been provided with the manuscript.

Declarations

Conflict of interest The authors have no conflict of interest to declare.

References

Abraham, M.J., Murtola, T., Schulz, R., Páll, S., Smith, J.C., Hess, B., Lindah, E.: GROMACS: High performance molecular simulations through multi-level parallelism from laptops to supercomputers. SoftwareX **1–2**, 19–25 (2015). https://doi.org/10.1016/J.SOFTX.2015.06.001

Ahmad, S., Gromiha, M.M., Fawareh, H., Sarai, A.: ASAView: Database and tool for solvent accessibility representation in proteins. BMC Bioinform. **5**(1), 1–5 (2004). https://doi.org/10.1186/1471-2105-5-51/FIGURES/1

Ahmed, S., Bhasin, M., Manjunath, K., Varadarajan, R.: Prediction of residue-specific contributions to binding and thermal stability using yeast surface display. Front. Mol. Biosci. **8**, 1336 (2022). https://doi.org/10.3389/FMOLB.2021.800819/BIBTEX

Amir, M., Mohammad, T., Kumar, V., Alajmi, M.F., Rehman, M.T., Hussain, A., Hassan, M.I.: Structural analysis and conformational dynamics of STN1 gene mutations involved in coat plus syndrome. Front. Mol. Biosci. (2019). https://doi.org/10.3389/FMOLB.2019.00041/BIBTEX

Berendsen, H.J.C., van der Spoel, D., van Drunen, R.: Gromacs—a message-passing parallel molecular-dynamics implementation. Comput. Phys. Commun. **91**(1–3), 43–56 (1995). https://doi.org/10.1016/0010-4655(95)00042-E

Brewer, M.K., Machio-Castello, M., Viana, R., Wayne, J.L., Kuchtová, A., Simmons, Z.R., Gentry, M.S.: An empirical pipeline for personalized diagnosis of Lafora disease mutations. Iscience (2021). https://doi.org/10.1016/j.isci.2021.103276

Chaki, M., Sengupta, M., Mondal, M., Bhattacharya, A., Mallick, S., Ray, K.: Molecular and Functional Studies of Tyrosinase Variants Among Indian Oculocutaneous Albinism Type 1 Patients. J. Invest. Dermatol. **131**(1) 260–262 (2011). https://doi.org/10.1038/jid.2010.274

Chen, V.B., Arendall, W.B., Headd, J.J., Keedy, D.A., Immormino, R.M., Kapral, G.J., Richardson, D.C.: MolProbity: all-atom structure validation for macromolecular crystallography. Acta Crystallogr. Sect. D: Biol. Crystallogr. (2010). https://doi.org/10.1107/S0907444909042073

Chou, P.Y., Fasman, G.D.: Prediction of protein conformation. Biochemistry **13**(2), 222–245 (1974). https://doi.org/10.1021/bi00699a002

Francis, E., Wang, N., Parag, H., Halaban, R., Hebert, D. N.: Tyrosinase Maturation and Oligomerization in the Endoplasmic Reticulum Require a Melanocyte-specific Factor J. Biol. Chem. **278**(28) 25607-25617 (2003). https://doi.org/10.1074/jbc.M303411200

Garnier, J., Osguthorpe, D.J., Robson, B.: Analysis of the accuracy and implications of simple methods for predicting the secondary structure of globular proteins. J. Mol. Biol. **120**(1), 97–120 (1978). https://doi.org/10.1016/0022-2836(78)90297-8

Guex, N., Peitsch, M.C.: SWISS-MODEL and the Swiss-PdbViewer: an environment for comparative protein modeling. Electrophoresis **18**(15), 2714–2723 (1997). https://doi.org/10.1002/ELPS.1150181505

Halaban, R., Cheng, E., Hebert, D. N.: Coexpression of Wild-Type Tyrosinase Enhances Maturation of Temperature-Sensitive Tyrosinase Mutants. J. Invest. Dermatol. **119**(2), 481–488 (2002). https://doi.org/10.1046/j.1523-1747.2002.01824.x

Halaban, R., Cheng, E., Zhang, Y., Moellmann, G., Hanlon, D., Michalak, M., Setaluri, V., Hebert, D.N.: Aberrant retention of tyrosinase in the endoplasmic reticulum mediates accelerated degradation of the enzyme and contributes to the dedifferentiated phenotype of amelanotic melanoma cells. Proc. Natl. Acad. Sci. **94**(12), 6210–6215 (1997). https://doi.org/10.1073/pnas.94.12.6210

Halaban, R., Svedine, S., Cheng, E., Smicun, Y., Aron, R., Hebert, D. N.: Endoplasmic reticulum retention is a common defect associated with tyrosinase-negative albinism. Proc. Natl. Acad. Sci. **97**(11), 5889–5894 (2000). https://doi.org/10.1073/pnas.97.11.5889

Kamaraj, B., Purohit, R.: In Silico screening and molecular dynamics simulation of disease-associated nsSNP in TYRP1 gene and its structural consequences in OCA3. BioMed Res. Int. (2013). https://doi.org/10.1155/2013/697051

Kufareva, I., Abagyan, R.: Methods of protein structure comparison. Methods Mol. Biol. **857**, 231 (2012). https://doi.org/10.1007/978-1-61779-588-6_10

Mondal, M., Sengupta, M., Ray, K.: Functional assessment of tyrosinase variants identified in individuals with albinism is essential for unequivocal determination of genotype-to-phenotype correlation. Br. J. Dermatol. **175**(6) 1232–1242 (2016). https://doi.org/10.1111/bjd.14977

Parthiban, V., Gromiha, M.M., Schomburg, D.: CUPSAT: prediction of protein stability upon point mutations. Nucleic Acids Res. (2006). https://doi.org/10.1093/NAR/GKL190

Pettersen, E.F., Goddard, T.D., Huang, C.C., Couch, G.S., Greenblatt, D.M., Meng, E.C., Ferrin, T.E.: UCSF Chimera—a visualization system for exploratory research and analysis. J. Comput. Chem. **25**(13), 1605–1612 (2004). https://doi.org/10.1002/JCC.20084

Ray, K., Chaki, M., Sengupta, M.: Tyrosinase and ocular diseases: Some novel thoughts on the molecular basis of oculocutaneous albinism type 1. Prog. Retin. Eye Res. **26**(4), 323–358 (2007). https://doi.org/10.1016/j.preteyeres.2007.01.001

Sarkar, D., Ray, K., Sengupta, M.: Structure-function correlation analysis of connexin50 missense mutations causing congenital cataract: electrostatic potential alteration could determine intracellular trafficking fate of mutants. BioMed Res. Int. (2014). https://doi.org/10.1155/2014/673895

Seifi, M., Walter, M.A.: Accurate prediction of functional, structural, and stability changes in PITX2 mutations using in silico bioinformatics algorithms. PLoS ONE **13**(4), e0195971 (2018). https://doi.org/10.1371/JOURNAL.PONE.0195971

Sengupta, M., Sarkar, D., Ganguly, K., Sengupta, D., Bhaskar, S., Ray, K.: In silico analyses of missense mutations in coagulation factor VIII: identification of severity determinants of haemophilia A. Haemophilia **21**(5), 662–669 (2015). https://doi.org/10.1111/hae.12662

Shafie, A., Khan, S., Batra, S., Anjum, F., Mohammad, T., Alam, S., Hassan, M.I.: Investigating single amino acid substitutions in PIM1 kinase: a structural genomics approach. PLoS ONE **16**(10), e0258929 (2021). https://doi.org/10.1371/JOURNAL.PONE.0258929

Toyofuku, K., Wada, I., Valencia, J. C., Kushimoto, T., Ferrans, V. J., Hearing, V. J.: Oculocutaneous albinism types 1 and 3 are ER retention diseases: mutation of tyrosinase or Tyrp1 can affect the processing of both mutant and wild-type proteins. FASEB J. **15**(12), 2149–2161 (2001). https://doi.org/10.1096/fsb2.v15.12 10.1096/fj.01-0216com

Webb, B., Sali, A.: Comparative protein structure modeling using modeller. Curr. Protocols in Bioinform. **54**, 561–5637 (2016). https://doi.org/10.1002/CPBI.3